Published in final edited form as:
J Neurol. 2012 June ; 259(6): 1199–1205. doi:10.1007/s00415-011-6337-x.

Decreased microglial activation in MS patients treated with glatiramer acetate

John N. Ratchford[1], **Christopher J. Endres**[2], **Dima A. Hammoud**[2], **Martin G. Pomper**[2], **Navid Shiee**[2], **John McGready**[3], **Dzung L. Pham**[4,5], and **Peter A. Calabresi**[1]

[1]Johns Hopkins University School of Medicine, Department of Neurology, Baltimore, Maryland, USA

[2]Johns Hopkins University School of Medicine, Department of Radiology, Baltimore, Maryland, USA

[3]Johns Hopkins Bloomberg School of Public Health, Department of Biostatistics, Baltimore, Maryland, USA

[4]Johns Hopkins University Department of Electrical Engineering, Baltimore, Maryland, USA

[5]Henry Jackson Foundation, Center for Neuroscience and Regenerative Medicine, Bethesda, Maryland, USA

Abstract

Activated microglia are thought to be an important contributor to tissue damage in multiple sclerosis (MS). The level of microglial activation can be measured non-invasively using [^{11}C]-*R*-PK11195, a radiopharmaceutical for positron emission tomography (PET). Prior studies have identified abnormalities in the level of [^{11}C]-*R*-PK11195 uptake in patients with MS, but treatment effects have not been evaluated. Nine previously untreated relapsing-remitting MS patients underwent PET and magnetic resonance imaging (MRI) of the brain at baseline and after one year of treatment with glatiramer acetate. Parametric maps of [^{11}C]-*R*-PK11195 uptake were obtained for baseline and post-treatment PET scans, and the change in [^{11}C]-*R*-PK11195 uptake pre- to post-treatment was evaluated across the whole brain. Region of interest analysis was also applied to selected subregions. Whole brain [^{11}C]-*R*-PK11195 binding potential per unit volume decreased 3.17% (95% CI: −0.74%, −5.53%) between baseline and one year ($p = 0.018$). A significant decrease was noted in cortical gray matter and cerebral white matter, and a trend towards decreased uptake was seen in the putamen and thalamus. The results are consistent with a reduction in inflammation due to treatment with glatiramer acetate, though a larger controlled study would be required to prove that association. Future research will focus on whether the level

Corresponding Author: John N. Ratchford, MD, Johns Hopkins University School of Medicine, 600 North Wolfe St., Pathology 627, Baltimore, MD 21287-6985, USA, Phone: 410-614-5835, Fax: 410-502-6736.

Disclosures

Dr. Ratchford receives research support from the Nancy Davis Foundation for Multiple Sclerosis and support for clinical trials from Novartis and Biogen Idec.
Dr. Endres has nothing to disclose.
Dr. Hammoud has nothing to disclose.
Dr. Pomper has nothing to disclose.
Mr. Shiee has nothing to disclose.
Dr. McGready has nothing to disclose.
Dr. Pham has nothing to disclose
Dr. Calabresi has received personal compensation for consulting, serving on scientific advisory boards and speaking activities from Biogen-IDEC, Teva, Merck-Serono, Novartis, Vertex, Vaccinex, Genzyme, and Abbott. He has received research funding from Biogen-IDEC, Teva, EMD-Serono, Vertex, Genentech, Abbott and Bayer.

of baseline microglial activation predicts future tissue damage in MS and whether [^{11}C]-*R*-PK11195 uptake in cortical gray matter correlates with cortical lesion load.

Keywords

multiple sclerosis; positron emission tomography; microglia; copolymer 1; immunology; PK11195

Introduction

Multiple sclerosis (MS) is a disease characterized pathologically by inflammatory demyelination and axonal transection in the central nervous system (CNS) [1]. In MS, autoreactive T cells are believed to enter the CNS and initiate an inflammatory response against autoantigens. Microglia make up about 10% of the cells of the brain, where they act as the resident macrophages by phagocytosing cellular debris and presenting foreign antigens [2]. Though microglia have an important role in CNS immunosurveillance, activation of microglia has also been implicated in the pathogenesis of a number of neurologic diseases. Inflammation in the CNS can both activate microglia and stimulate migration of monocytes from the vasculature into the CNS, where they can then differentiate into macrophages (reviewed in [3] and [4]. Microglia have the potential to activate perivascular myelin-reactive T cells through antigen presentation [5]. In MS and experimental allergic encephalomyelitis (EAE), an animal model of MS, microglial activation contributes to CNS tissue damage through production of proinflammatory cytokines, matrix metalloproteinases, and free radicals (reviewed in [6]). In EAE, areas of demyelination have high numbers of microglia [7] and depletion of either macrophages or microglia leads to marked attenuation of EAE even in the presence of adequate T cell sensitization [8, 9]. This has led some to propose that microglia are the primary effectors of tissue damage in MS [10].

Following brain injury, activated microglia express higher levels of the translocator protein 18 kDa (TSPO, formerly called the peripheral benzodiazepine receptor) [11–14]. This protein is present on the outer mitochondrial membrane and is involved in a number of cellular processes [15]. [^{11}C]-*R*-PK11195 is a radiopharmaceutical for positron emission tomography (PET) that binds to TSPO (reviewed in [16]), which is a marker for microglial activation. Higher levels of TSPO will cause increased binding and slower clearance of [^{11}C]-*R*-PK11195. Healthy brain has low TSPO levels and thus shows minimal uptake of [^{11}C]-*R*-PK11195.

A post-mortem study of brain tissue from MS patients found increased [^{3}H]-*R*-PK11195 binding in MS plaques, and PET imaging of twelve MS patients found increased [^{11}C]-*R*-PK11195 binding in gadolinium-enhancing lesions and in the normal-appearing brainstem and thalamus [14]. Moreover, that PET study found that [^{11}C]-*R*-PK11195 binding increased in lesions during a relapse [14]. Another study of [^{11}C]-PK11195 PET in MS found a significant increase in uptake in gadolinium-enhancing lesions and a trend towards decreased uptake in T2 hyperintense lesions [17]. This study also found that [^{11}C]-PK11195 uptake increased during relapses and that an increase in normal-appearing white matter (NAWM) was associated with disease progression. However, this study did not find a difference in PK11195 uptake in normal-appearing white matter or gray matter between MS patients and controls. A third study found an association between [^{11}C]-PK11195 uptake in NAWM and brain atrophy, suggesting that atrophy could be a consequence of microglia-mediated inflammation in NAWM [18]. Also, the degree of microglial activation in cortical gray matter was found to be greater in patients with secondary progressive MS than relapsing-remitting MS [19] and disease duration had a positive correlation with microglial

activation [17, 20]. While two studies have noted that [^{11}C]-PK11195 binding is higher during relapses, the effect of MS treatment on [^{11}C]-PK11195 binding and microglial activation has not been studied. We performed a longitudinal cohort study of MS patients initiating glatiramer acetate (Copaxone, Teva Pharmaceuticals, Petach Tikva, Israel) treatment in order to evaluate whether microglial activation, as measured by [^{11}C]-*R*-PK11195 uptake, is affected by treatment. In an exploratory analysis we also investigated whether the degree of baseline microglial activation is associated with the rate of brain atrophy.

Methods

Patients

Nine patients with relapsing-remitting MS (RRMS) who were initiating treatment with glatiramer acetate 20 mg subcutaneous injection daily were recruited from a single center. Diagnosis was determined using the revised McDonald criteria [21]. Disease duration was calculated as the time from the first demyelinating event to the first PET scan. All participants provided written informed consent after the experimental nature of the study was explained. The study was approved by the local Institutional Review Board and was performed in compliance with the Code of Ethics of the World Medical Association (Declaration of Helsinki). Exclusion criteria were age <18 years, inability to tolerate MRI, and current or desired pregnancy in the year following study enrollment. All nine patients completed the study.

MRI

Study subjects underwent an MRI prior to and after one year of treatment. A gadolinium-enhanced brain MRI was acquired using a 3.0-T Philips scanner and a three-dimensional SPGR (spoiled gradient recalled acquisition in the steady state) sequence with the following parameters: echo train = 154, relaxation time = 10.2 ms, echo time = 6 ms, flip angle = 8 degrees, field of view = 21.2 × 21.2 cm, slice thickness = 1.17 mm, and reconstruction matrix of 256 × 256, yielding an in-plane pixel size of 0.83 × 0.83 mm. MRI scans were performed on the same day as the PET scan.

The lesion-TOADS software (part of TOADS-CRUISE software package; available as a software plug-in to the Medical Image Processing, Analysis, and Visualization (MIPAV) software package, http://www.nitrc.org/projects/toads-cruise/) was used to measure the volume of the brain and its substructures. Details regarding this program are described elsewhere [22], but briefly the program utilizes a statistical atlas and a topological atlas that are rigidly registered to the MR image. In a multi-step process the program delineates and measures the following regions of interest (ROIs): cerebral white matter, cortical gray matter, caudate, thalamus, putamen, cerebellar gray matter, cerebellar white matter, brainstem, and ventricular volume. The program is also able to identify and measure T2 lesions. The ROI maps from these MRI images were then transformed into the parametric PET space by means of a rigid registration so that the uptake of radiotracer could be measured in individual regions.

PET

Subjects underwent a PET scan of the brain prior and after one year of glatiramer acetate treatment. PET images were acquired on a CPS/CTI High Resolution Research Tomograph (HRRT), head-only camera, with axial spatial resolution (FWHM) of 2.4 mm, and an in-plane resolution of 2.4 – 2.8 mm. This scanner acquires 207 simultaneous slices of 1.22 mm thickness. The axial and transaxial fields of view are 24.0 cm and 31.2 cm, respectively. To calculate an attenuation correction for the emission scans, a six minute transmission scan

was obtained with a ^{137}CS source (energy = 662 keV), prior to radiopharmaceutical injection. The attenuation map obtained with ^{137}CS is converted using a lookup table to estimate attenuation coefficients for 511 keV photons. [^{11}C]-*R*-PK11195 (686 ± 43 MBq; 414 ± 272 GBq/μmol) was delivered *via* intravenous bolus injection. Dynamic PET studies consisted of a 19 frame protocol (3 × 20 sec, 2 × 30 sec, 2 × 60 sec, 3 × 120 sec, 8×300 sec, 1 × 600 sec) with a total scan duration of 60 minutes. PET scans were reconstructed using ordered-subsets expectation-maximum (OSEM) reconstruction, in a 31×31 cm field of view and a 256×256 pixel matrix with a pixel size of 1.2 × 1.2 mm. PET frames were corrected for radioactive decay to the initial PET frame. A thermoplastic mask was fitted to each subject's face for the purpose of immobilization and positioning during scanning. To correct for small head movements, the PET frames from 6 minutes until the end of the study were realigned to an early mean image created by averaging the frames from 2–10 minutes. This motion correction procedure was performed using the normalized mutual information method and the realign function in SPM5 (Wellcome Department of Cognitive Neurology, London, UK). After realignment of the image frames, a mean PET image (20–60 minutes) was used for MR-PET coregistration. MR scans were used to identify the ROIs described above, which were then transferred to the dynamic PET data to generate tissue time-activity curves. ANALYZE software (Mayo Foundation, Rochester, MN) was used for processing ROIs and time-activity curves (TACs).

Data Analysis and Statistics

There is no brain region that is devoid of TSPO, although it has been shown that a cerebellum reference may add stability to quantitative analyses [23]. It was noted that no lesions were present in the cerebella of these subjects. Using the cerebellar gray matter time activity curve as input, a bilinear form of the reference region Logan method [24] was applied to produce parametric images of the binding potential relative to nondisplaceable ligand (BP_{ND}). The BP_{ND} images before (BP_{ND1}) and after treatment (BP_{ND2}) were coregistered to the initial (pre-treatment) T1 weighted MR, then in MR space a difference BP_{ND} map ΔBP_{ND} = (BP_{ND1} - BP_{ND2}) was created to examine decreases in binding from pre- to post-treatment. Similarly, the reverse contrast = (BP_{ND2} - BP_{ND1}) was used to examine possible increases in binding. The pre-treatment MR scans were used to create a normalization template using the DARTEL procedure [25] implemented in SPM8 (http://www.fil.ion.ucl.ac.uk/spm/). Subsequently, images of ΔBP_{ND} were normalized to the Montreal Neurological Institute Atlas for statistical comparison with SPM8 (Wellcome Department of Cognitive Neurology, London, United Kingdom).

Both ROI and voxel-based analyses were used. For each PET study, parametric images of BP_{ND} were generated. The first analysis technique calculated the mean uptake of [^{11}C]-*R*-PK11195 per voxel in a given brain region. Baseline and year one results were compared using a paired t-test. The Wilcoxon signed-rank test was also used and showed the same results as the paired t-test. Analyses were performed using STATA version 10.0 (StataCorp, College Station, Texas). For the comparison of regional [^{11}C]-*R*-PK11195 uptake, statistical significance was defined as $p < 0.05$. The second analysis method used the statistical parametric mapping (SPM) technique described above to identify regions where there was a significant change from baseline to year one. A one-sample t-test with alpha (rejection level) = 0.005 was used to identify regions that had decreased (or increased) [^{11}C]-*R*-PK11195 uptake in the SPM analysis.

Results

Nine untreated patients with RRMS starting glatiramer acetate treatment were enrolled in the study. Demographic data are shown in Table I. All participants underwent PET and MRI scans at baseline before initiating glatiramer acetate and again after one year of treatment.

The mean time between PET scans was 392 days (range 354 – 461 days). All participants were relapse-free for at least one month before the initial PET scan (median = 6 months, range 1 – 42 months) and none had been treated with corticosteroids for at least one month. There was no evidence of an association between disease duration and baseline [^{11}C]-*R*-PK11195 uptake, although a modest association would be difficult to detect given the small sample size. Eight of the nine patients had no clinical relapses during the one year study period. One of the nine patients experienced two relapses during the study period and was changed from glatiramer acetate to natalizumab by their physician. Interestingly, this active patient had the highest [^{11}C]-*R*-PK11195 binding potential on the baseline PET scan, suggesting that this measure may have some prognostic significance. The data were analyzed both including and excluding data from the one patient who changed to natalizumab. The results were the same both ways, and ultimately that patient's follow-up data were excluded from the final analyses to minimize the treatment discrepancy. The mean change in whole brain volume over the one year study was −0.8% ($p = 0.06$). Median baseline Expanded Disability Status Scale Score was 2.0 (range 1.0 – 6.0) and was unchanged at the end of the study. The mean T2 lesion volume was relatively low at baseline (3.93 mL) and increased by 11% during the study, although this increase was not statistically significant. Baseline [^{11}C]-*R*-PK11195 binding potential was not associated with T2 lesion volume in this small cohort.

For comparison of pre- and post-treatment results, there were no significant differences in injected dose (677 ± 53, 685 ± 26 MBq), tracer mass (0.88 ± 0.83, 0.70 ± 0.21 μg), specific activity (472 ± 398, 375 ± 11 GBq/ μmol), or subject weight (74.4 ± 12.9, 75.5 ± 15.2 kg) ($p > 0.05$ using a paired t-test). The percent change in [^{11}C]-*R*-PK11195 in each brain region between baseline and one year post-treatment is shown in Table II. Whole brain [^{11}C]-*R*-PK11195 binding potential per unit volume decreased 3.17% (95% CI: −0.74%, −5.53%) between baseline and one year ($p = 0.018$, Figure 1a). [^{11}C]-*R*-PK11195 binding potential per unit volume decreased in the following regions: supratentorial brain, infratentorial brain, cerebral white matter, cortical gray matter, thalamus, and putamen. No notable change was observed in the caudate. The drop in [^{11}C]-*R*-PK11195 binding potential was statistically significant in cortical gray matter (−3.35%, 95% CI: −1.39%, −5.26%, Figure 1b) and cerebral white matter (−3.25%, 95% CI: −0.08%, −6.36%, Figure 1c). There also was a trend towards lower [^{11}C]-*R*-PK11195 binding potential in the putamen and thalamus ($p <= 0.10$). T2 hyperintense lesions showed no significant change in [^{11}C]-*R*-PK11195 binding potential between baseline and one year.

Baseline binding potential was greater in gray matter than in white matter (ratio = 1.19, $p < 0.0001$), likely due to more blood flow to gray matter and a greater concentration of microglia in gray matter [26]. We analyzed whether there was a greater change in [^{11}C]-*R*-PK11195 binding potential in gray matter or white matter structures. The rate of change was similar in the cortical gray matter and cerebral white matter (−3.35% vs. −3.25%, $p = 0.33$). This suggests that the drop in microglial activation is a more global effect and was not specific to gray or white matter. We also evaluated whether the baseline level of [^{11}C]-*R*-PK11195 binding potential predicted rate of brain atrophy over the subsequent year. No definite association could be identified (data not shown), though the study was not powered to demonstrate such an association.

A statistical parametric mapping technique was also used to evaluate change in [^{11}C]-*R*-PK11195 uptake. This technique merged the individual data and identified areas with a significant change in uptake. Areas of decreased uptake were identified, predominantly in the cortical gray matter (Figure 2). Based on the ROI analysis the change in [^{11}C]-*R*-PK11195 uptake was relatively global, but the areas highlighted in the example in Figure 2

represent areas where there was the most dramatic drop in tracer uptake between baseline and year 1.

Discussion

This study used [^{11}C]-*R*-PK11195 binding to measure the degree of microglial activation in patients before and after treatment with glatiramer acetate. Whole brain [^{11}C]-*R*-PK11195 binding potential decreased modestly after treatment with glatiramer acetate, which was reflected both in white matter and gray matter structures. Based on the SPM analysis, the most prominent changes occurred in the cortical gray matter. The mechanism of action of glatiramer acetate is not fully understood, though it is hypothesized to inhibit the activation of myelin basic protein-reactive T cells and to induce immunomodulatory Th2 cells [27]. Since microglia have been recognized as an important contributor to tissue damage and disease progression in MS [10], it is possible that part of the beneficial effect of glatiramer acetate in MS is derived from an effect on microglia. Indeed, glatiramer acetate has been found to have direct effects on microglia, promoting differentiation of monocytes and microglia into antigen-presenting cells [28] and stimulating phagocytosis by microglia *in vitro* [29].

It is difficult to compare our results with prior PK11195 MS studies, as they primarily focused more the differences between MS brains and controls, and the difference between normal-appearing brain and lesions, whereas our study evaluated longitudinal change in MS patients only. However, a single subject in a prior study was scanned both during and four months after a relapse and a notable decrease in [^{11}C]-*R*-PK11195 binding potential was noted [17]; this would be consistent with our finding of decreased binding potential in patients who initiate immunomodulatory treatment. Since patients were specifically scanned during periods of disease remission, we were not able to evaluate previous findings of an increase in [^{11}C]-*R*-PK11195 binding potential during a relapse. It is of interest that the patient with the most relapse activity during our study had the highest baseline [^{11}C]-*R*-PK11195 binding potential. This suggests the possibility that [^{11}C]-*R*-PK11195 might have utility for predicting relapse activity, though this could not be proven due to the low level of disease activity seen in this cohort. No definite association between baseline [^{11}C]-*R*-PK11195 binding potential and brain atrophy rate could be demonstrated, though the study was not powered for such an analysis.

This study has several limitations. The first limitation is the relatively small sample size, which largely is due to the high cost associated with PET. Though the observed decreases in microglial activation were statistically significant, it is unknown whether they are clinically meaningful. A larger cohort study would be needed to identify an association between clinical outcomes (e.g. relapse rate) and change in microglial activation or to evaluate the prognostic utility of scanning with [^{11}C]-*R*-PK11195 or similar PET radiotracers. A second limitation is the lack of an untreated control group. In order to conclude that glatiramer acetate was the cause of the decrease in [^{11}C]-*R*-PK11195 binding potential, it would have been necessary also to follow an untreated cohort of RRMS patients and demonstrate no change in that group. For ethical reasons this was not done, so it cannot be concluded definitively that glatiramer acetate was the cause of the decrease in [^{11}C]-*R*-PK11195 binding potential. An alternative explanation is that this modest decrease in microglial activation was due to the natural history of the disease, although that would be inconsistent with previous findings that microglial activation increases with disease duration in MS [17, 20]. Another potential limitation is that using the cerebellum as a reference region may lead to an underestimate of the change in binding potential, since some specific binding does occur in that region.

PET scanning is a promising technology for understanding MS pathogenesis. Since the prognosis in MS is widely variable, one of the major challenges in MS management is predicting an individual's risk of developing disability. Although relapses are an important contributor to disability, much of the disability also likely accrues from axonal and neuronal damage that is initially subclinical. Measuring the baseline level of microglial activation has the potential to be a useful tool for predicting future tissue damage and understanding treatment effects. Although this study was underpowered to evaluate this, future studies could address whether baseline microglial activation predicts change in brain volume, a marker of axonal damage. Our study identified significant microglial activation in the cortical gray matter of MS patients and there is currently great interest in understanding the etiology of cortical lesions in MS. Microglia may have an important effect on the development of cortical lesions. Indeed, when activated, cortical microglia have been found to migrate to and strip synapses from neurons [30]. TSPO tracers may prove to be a useful tool to study the pathogenesis of cortical lesions. Furthermore, there is evidence that mitochondrial dysfunction may lead to degeneration of chronically demyelinated axons [31]. Since TSPO is found in mitochondria, changes in TSPO levels may reflect this mitochondrial dysfunction. Newer radiotracers such as [^{11}C]-DPA-713 [32], [^{11}C]-PBR28 [20], and [^{11}C]-DAA1106 [33] have higher affinity for TSPO as well as other positive attributes, and future studies of microglial function in MS will likely utilize these newer ligands.

Acknowledgments

This study was funded by an independent medical grant from TEVA Neuroscience to Dr. Calabresi. The study sponsor had no role in the design or execution of the study, data analysis, manuscript preparation, or decision to submit the paper for publication.

References

1. Trapp BD, Peterson J, Ransohoff RM, Rudick R, Mork S, Bo L. Axonal transection in the lesions of multiple sclerosis. N Engl J Med. 1998; 338:278–285. [PubMed: 9445407]
2. Perry VH, Gordon S. Macrophages and the nervous system. Int Rev Cytol. 1991; 125:203–244. [PubMed: 1851730]
3. Guillemin GJ, Brew BJ. Microglia, macrophages, perivascular macrophages, and pericytes: a review of function and identification. J Leukoc Biol. 2004; 75:388–397. [PubMed: 14612429]
4. Gehrmann J, Matsumoto Y, Kreutzberg GW. Microglia: intrinsic immuneffector cell of the brain. Brain Res Brain Res Rev. 1995; 20:269–287. [PubMed: 7550361]
5. Dangond F, Windhagen A, Groves CJ, Hafler DA. Constitutive expression of costimulatory molecules by human microglia and its relevance to CNS autoimmunity. J Neuroimmunol. 1997; 76:132–138. [PubMed: 9184642]
6. Benveniste EN. Role of macrophages/microglia in multiple sclerosis and experimental allergic encephalomyelitis. J Mol Med. 1997; 75:165–173. [PubMed: 9106073]
7. Bauer J, Sminia T, Wouterlood FG, Dijkstra CD. Phagocytic activity of macrophages and microglial cells during the course of acute and chronic relapsing experimental autoimmune encephalomyelitis. J Neurosci Res. 1994; 38:365–375. [PubMed: 7932870]
8. Brosnan CF, Bornstein MB, Bloom BR. The effects of macrophage depletion on the clinical and pathologic expression of experimental allergic encephalomyelitis. J Immunol. 1981; 126:614–620. [PubMed: 6256443]
9. Huitinga I, van Rooijen N, de Groot CJ, Uitdehaag BM, Dijkstra CD. Suppression of experimental allergic encephalomyelitis in Lewis rats after elimination of macrophages. J Exp Med. 1990; 172:1025–1033. [PubMed: 2145387]
10. Sriram S, Rodriguez M. Indictment of the microglia as the villain in multiple sclerosis. Neurology. 1997; 48:464–470. [PubMed: 9040740]

11. Dubois A, Benavides J, Peny B, Duverger D, Fage D, Gotti B, MacKenzie ET, Scatton B. Imaging of primary and remote ischaemic and excitotoxic brain lesions. An autoradiographic study of peripheral type benzodiazepine binding sites in the rat and cat. Brain Res. 1988; 445:77–90. [PubMed: 2835123]
12. Myers R, Manjil LG, Cullen BM, Price GW, Frackowiak RS, Cremer JE. Macrophage and astrocyte populations in relation to [3H]PK 11195 binding in rat cerebral cortex following a local ischaemic lesion. J Cereb Blood Flow Metab. 1991; 11:314–322. [PubMed: 1997503]
13. Banati RB, Myers R, Kreutzberg GW. PK ('peripheral benzodiazepine')--binding sites in the CNS indicate early and discrete brain lesions: microautoradiographic detection of [3H]PK11195 binding to activated microglia. J Neurocytol. 1997; 26:77–82. [PubMed: 9181482]
14. Banati RB, Newcombe J, Gunn RN, Cagnin A, Turkheimer F, Heppner F, Price G, Wegner F, Giovannoni G, Miller DH, Perkin GD, Smith T, Hewson AK, Bydder G, Kreutzberg GW, Jones T, Cuzner ML, Myers R. The peripheral benzodiazepine binding site in the brain in multiple sclerosis: quantitative in vivo imaging of microglia as a measure of disease activity. Brain. 2000; 123(Pt 11):2321–2337. [PubMed: 11050032]
15. Casellas P, Galiegue S, Basile AS. Peripheral benzodiazepine receptors and mitochondrial function. Neurochem Int. 2002; 40:475–486. [PubMed: 11850104]
16. Venneti S, Lopresti BJ, Wiley CA. The peripheral benzodiazepine receptor (Translocator protein 18kDa) in microglia: from pathology to imaging. Prog Neurobiol. 2006; 80:308–322. [PubMed: 17156911]
17. Debruyne JC, Versijpt J, Van Laere KJ, De Vos F, Keppens J, Strijckmans K, Achten E, Slegers G, Dierckx RA, Korf J, De Reuck JL. PET visualization of microglia in multiple sclerosis patients using [11C]PK11195. Eur J Neurol. 2003; 10:257–264. [PubMed: 12752399]
18. Versijpt J, Debruyne JC, Van Laere KJ, De Vos F, Keppens J, Strijckmans K, Achten E, Slegers G, Dierckx RA, Korf J, De Reuck JL. Microglial imaging with positron emission tomography and atrophy measurements with magnetic resonance imaging in multiple sclerosis: a correlative study. Mult Scler. 2005; 11:127–134. [PubMed: 15794383]
19. Politis M, Giannetti P, Su P, Turkheimer F, Keihaninejad S, Wu K, Waldman A, Reynolds R, Nicholas R, Piccini P. Cortical microglial activation is associated with disability in secondary progressive multiple sclerosis: an in vivo imaging study. Neurology. 2010; 74:A290.
20. Oh U, Fujita M, Ikonomidou VN, Evangelou IE, Matsuura E, Harberts E, Ohayon J, Pike VW, Zhang Y, Zoghbi SS, Innis RB, Jacobson S. Translocator Protein PET Imaging for Glial Activation in Multiple Sclerosis. J Neuroimmune Pharmacol. 2010; 6:354–361. [PubMed: 20872081]
21. Polman CH, Reingold SC, Edan G, Filippi M, Hartung HP, Kappos L, Lublin FD, Metz LM, McFarland HF, O'Connor PW, Sandberg-Wollheim M, Thompson AJ, Weinshenker BG, Wolinsky JS. Diagnostic criteria for multiple sclerosis, 2005 revisions to the "McDonald Criteria". Ann Neurol. 2005; 58:840–846. [PubMed: 16283615]
22. Shiee N, Bazin PL, Ozturk A, Reich DS, Calabresi PA, Pham DL. A topology-preserving approach to the segmentation of brain images with multiple sclerosis lesions. Neuroimage. 2010; 49:1524–1535. [PubMed: 19766196]
23. Kropholler MA, Boellaard R, van Berckel BN, Schuitemaker A, Kloet RW, Lubberink MJ, Jonker C, Scheltens P, Lammertsma AA. Evaluation of reference regions for (R)-[(11)C]PK11195 studies in Alzheimer's disease and mild cognitive impairment. J Cereb Blood Flow Metab. 2007; 27:1965–1974. [PubMed: 17406654]
24. Logan J, Fowler JS, Volkow ND, Wang GJ, Ding YS, Alexoff DL. Distribution volume ratios without blood sampling from graphical analysis of PET data. J Cereb Blood Flow Metab. 1996; 16:834–840. [PubMed: 8784228]
25. Ashburner J. A fast diffeomorphic image registration algorithm. Neuroimage. 2007; 38:95–113. [PubMed: 17761438]
26. Lawson LJ, Perry VH, Dri P, Gordon S. Heterogeneity in the distribution and morphology of microglia in the normal adult mouse brain. Neuroscience. 1990; 39:151–170. [PubMed: 2089275]
27. Dhib-Jalbut S. Mechanisms of action of interferons and glatiramer acetate in multiple sclerosis. Neurology. 2002; 58:S3–S9. [PubMed: 11971121]

28. Kim HJ, Ifergan I, Antel JP, Seguin R, Duddy M, Lapierre Y, Jalili F, Bar-Or A. Type 2 monocyte and microglia differentiation mediated by glatiramer acetate therapy in patients with multiple sclerosis. J Immunol. 2004; 172:7144–7153. [PubMed: 15153538]

29. Pul R, Moharregh-Khiabani D, Skuljec J, Skripuletz T, Garde N, Voss EV, Stangel M. Glatiramer Acetate Modulates TNF-alpha and IL-10 Secretion in Microglia and Promotes Their Phagocytic Activity. J Neuroimmune Pharmacol. 2010; 6:381–388. [PubMed: 21046275]

30. Trapp BD, Wujek JR, Criste GA, Jalabi W, Yin X, Kidd GJ, Stohlman S, Ransohoff R. Evidence for synaptic stripping by cortical microglia. Glia. 2007; 55:360–368. [PubMed: 17136771]

31. Dutta R, McDonough J, Yin X, Peterson J, Chang A, Torres T, Gudz T, Macklin WB, Lewis DA, Fox RJ, Rudick R, Mirnics K, Trapp BD. Mitochondrial dysfunction as a cause of axonal degeneration in multiple sclerosis patients. Ann Neurol. 2006; 59:478–489. [PubMed: 16392116]

32. Endres CJ, Pomper MG, James M, Uzuner O, Hammoud DA, Watkins CC, Reynolds A, Hilton J, Dannals RF, Kassiou M. Initial evaluation of 11C-DPA-713, a novel TSPO PET ligand, in humans. J Nucl Med. 2009; 50:1276–1282. [PubMed: 19617321]

33. Ikoma Y, Yasuno F, Ito H, Suhara T, Ota M, Toyama H, Fujimura Y, Takano A, Maeda J, Zhang MR, Nakao R, Suzuki K. Quantitative analysis for estimating binding potential of the peripheral benzodiazepine receptor with [(11)C]DAA1106. J Cereb Blood Flow Metab. 2007; 27:173–184. [PubMed: 16685259]

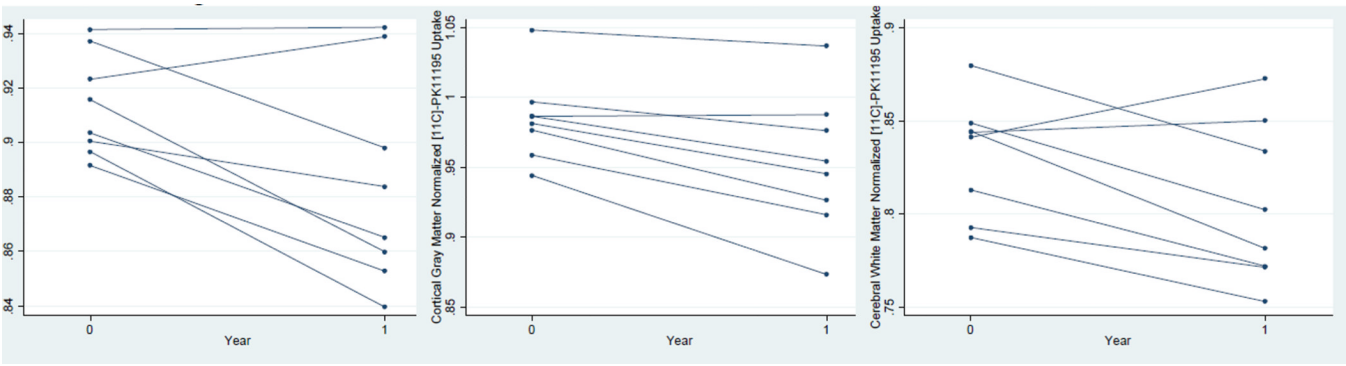

Figure 1.

Plot of change in [^{11}C]-*R*-PK11195 binding potential at baseline and year one for a) whole brain, b) cortical gray matter, and c) cerebral white matter. Each line represents an individual patient.

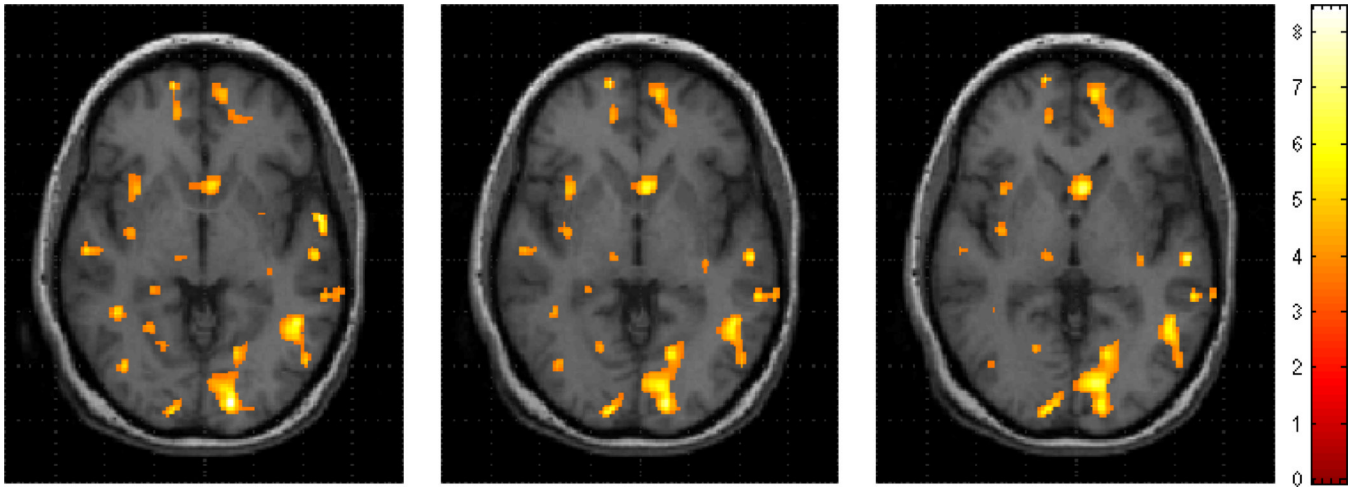

Figure 2.

Three representative axial T1-weighted brain MRI images with overlaid composite PET data from the SPM analysis. This represents the summary data from all patients. Areas where there was a drop in [^{11}C]-*R*-PK11195 uptake from baseline to follow-up MRI are highlighted (extent threshold = 10 voxels, $p = 0.005$). The color scale on the right represents t values. It is likely that there was a global effect and the highlighted areas demonstrated the most dramatic change.

Table I

Demographic data

	Patients
Number	9
Percent female	89%
Median age (range)	51 (25–62)
Median disease duration in years (range)	5.3 (0.5–21)
Baseline median Expanded Disability Status Scale Score (range)	2.0 (1.0 – 6.0)
One year median Expanded Disability Status Scale Score (range)	2.0 (1.0 – 6.0)

Table II

Percent change in [^{11}C]-R-PK11195 binding potential at baseline and after one year of glatiramer acetate treatment in the whole brain, substructures, and T2 lesions.

Region	Percent Change (95% CI)	*p*-value
Whole brain	−3.17 (−0.74, −5.53)	0.018
Supratentorial	−3.30 (−0.85, −5.65)	0.015
Infratentorial	−2.22 (0.51, −4.91)	0.096
Cerebral white matter	−3.25 (−0.08, −6.36)	0.046
Cortical gray matter	−3.35 (−1.39, −5.26)	0.0048
Caudate	0.142 (9.51, −9.36)	0.99
Thalamus	−3.63 (0.54, −7.80)	0.079
Putamen	−2.83 (0.71, −6.48)	0.10
T2 lesions	−0.416 (6.23, −7.05)	0.89